

Groundwater oxygen anomaly related to the 2016 Kumamoto earthquake in Southwest Japan

By Yuji SANO,^{*1,*2,†} Satoki ONDA,^{*1} Takanori KAGOSHIMA,^{*1} Toshihiro MIYAJIMA,^{*1}
Naoto TAKAHATA,^{*1} Tomo SHIBATA,^{*3} Chika NAKAGAWA,^{*4} Tetsuji ONOUE,^{*4,*5}
Nak Kyu KIM,^{*6} Hyunwoo LEE,^{*7} Minoru KUSAKABE^{*8} and Daniele L. PINTI^{*9}

(Edited by Yoshio FUKAO, M.J.A.)

Abstract: Here, we report the groundwater oxygen isotope anomalies caused by the 2016 Kumamoto earthquake (M_{JMA}7.3) that occurred in Southwest Japan on April 16, 2016. One hundred and seventeen groundwater samples were collected from a deep well located 3 km to the southeast of the epicenter in Mifune Town, Kumamoto Prefecture; they were drinking water packed in PET bottles and distributed in the area between April 2015 and March 2018. Further, the oxygen and hydrogen isotopes were evaluated via cavity ring-down spectroscopy without performing any pretreatment. An anomalous increase was observed with respect to the $\delta^{18}\text{O}$ value (up to 0.51‰) soon after the earthquake along with a precursory increase of 0.38‰ in January 2016 before the earthquake. During these periods, there was no noticeable change in the hydrogen isotopic ratios. Rapid crustal deformation related to the earthquake may have enhanced the microfracturing of the aquifer rocks and the production of new surfaces, inducing $\delta^{18}\text{O}$ enrichment via oxygen isotopic exchange between rock and porewater without changing $\delta^2\text{H}$.

Keywords: groundwater, earthquake precursors, hydrogen isotopes, oxygen isotopes, 2016 Kumamoto earthquake

1. Introduction

Earthquakes with large magnitudes are the worst among natural disasters, claiming many lives

and significantly damaging the infrastructure in both developed and developing countries. Therefore, such earthquakes should be predicted when scientifically and technically possible. The geochemical precursors of earthquakes have attracted the attention of researchers worldwide.^{1),2)} The chemistry of groundwater has been monitored to predict earthquakes in U.S.A., Japan, China, and Italy since the 1970s.^{3),4)} Even though the concentration anomalies of noble gases, such as radon (^{222}Rn) and helium (^4He), are well documented,^{1),5)} their geochemical behaviors that cause anomalous changes have not been considerably investigated.⁶⁾ Major criticism can be summarized as most signals are anecdotal with no statistical assessment⁷⁾ or fragmental with insufficient time series and lack of decisive data.⁸⁾ Several precursors did not meet the criteria for critical assessment.³⁾ Toward the end of the 1990s, a seismologist suggested that earthquakes were inherently unpredictable based on the results obtained by nonlinear dynamics.⁹⁾ Subsequently, the geoscientific community became pessimistic with respect to earthquake prediction. However, groundwater monitoring is still

^{*1} Atmosphere and Ocean Research Institute, The University of Tokyo, Kashiwa, Chiba, Japan.

^{*2} Institute of Surface-Earth System Science, Tianjin University, Tianjin, China.

^{*3} Institute for Geothermal Sciences, Kyoto University, Beppu, Oita, Japan.

^{*4} Department of Earth and Environmental Sciences, Kumamoto University, Kumamoto, Japan.

^{*5} Department of Earth and Planetary Sciences, Kyushu University, Fukuoka, Japan.

^{*6} Unit of Antarctic K-route Expedition, Korea Polar Research Institute, Incheon, Korea.

^{*7} School of Earth and Environmental Sciences, Seoul National University, Seoul, Korea.

^{*8} Department of Environmental Biology and Chemistry, Toyama University, Toyama, Japan.

^{*9} GEOTOP & Research Center on Earth System Dynamics, Université du Québec à Montréal, Montréal, QC, Canada.

† Correspondence should be addressed: Y. Sano, Atmosphere and Ocean Research Institute, The University of Tokyo, 5-1-5 Kashiwanoha, Kashiwa, Chiba 277-8564, Japan (e-mail: ysano@ori.u-tokyo.ac.jp).

performed because researchers believe that precursors are not entirely unexpected.^{1),2)}

In addition to radon,⁸⁾ helium,^{6),7)} sulfate (SO_4^-), and chlorine (Cl^-),¹⁰⁾ the possible variations of hydrogen ($^2\text{H}/^1\text{H}$ or $\delta^2\text{H}$) and oxygen ($^{18}\text{O}/^{16}\text{O}$ or $\delta^{18}\text{O}$) isotopic ratios in groundwater were discussed in seismically active regions.¹¹⁾ The hydrogeochemical changes associated with stable isotopes were reported before and after the occurrence of a M5.8 earthquake in Iceland.¹²⁾ Oxygen isotopic changes were detected contemporarily to the occurrence of a M5.1 earthquake in India, and a model¹³⁾ of aquifer breaching and mixing of different groundwater masses having different isotopic signatures was proposed. Complicated oxygen and hydrogen isotope changes were observed before and after two consecutive M5.5–5.6 earthquakes in Iceland,¹⁴⁾ and the isotopic anomalies can be attributed to the mixing of various types of groundwater. Conversely, a groundwater oxygen isotope anomaly was reported without any considerable hydrogen isotope change at the time of the M_{JMA}6.6 2016 Tottori earthquake that occurred in Southwest Japan.¹⁵⁾ This variation was interpreted as the ^{18}O shift caused by the water–rock interaction in a very short period of time,¹⁶⁾ which is a different mechanism that associated with the mixing of groundwater in Iceland^{12),14)} and India.¹³⁾

Even though oxygen and hydrogen anomalies are promising with respect to the prediction of earthquakes, more data are required to confirm the predictability and elucidate the mechanism that causes the mixing of different groundwater masses or the water–rock interaction. Here, we present the data of oxygen and hydrogen isotope changes in local groundwater related to the M_{JMA}7.3 2016 Kumamoto earthquake.

2. Experiment

Determining a suitable location to monitor the groundwater characteristics before the occurrence of a major earthquake is difficult because we do not know when and where the earthquake will occur. Therefore, an observation groundwater well located close to the epicenter can be selected after the earthquake. Obviously, it is impossible to collect pre-earthquake groundwater samples from this well after the earthquake because the water dissipates in the well and/or into the aquifer. However, if this well is used for producing commercial bottled mineral water, then it can be used as a unique archive for monitoring geochemical anomalies. Commercial water has a precise production date, and its content

is chemically well preserved,¹⁰⁾ except for helium because this inert gas permeates and escapes quickly through either plastic or glass bottles. Companies often store the mineral water samples obtained well before the earthquake for quality management purposes. Generally, mineral water samples can be stored for only one year because of the legal expiration date restrictions in Japan. Thus, the fragmentation of data in time series can be avoided. We have collected commercial bottled mineral water samples from the Takagi site in Kumamoto Prefecture, central Kyushu Island, Southwest Japan (Fig. 1) one year before and two years after the earthquake. This method is similar to that used by Tsunogai and Wakita, who reported chemical changes in groundwater before and after the M_{JMA}7.0 Kobe earthquake in 1995.¹⁰⁾

The 2016 Kumamoto earthquake sequence includes three large seismic events ($M_{\text{JMA}} > 6$) that occurred on the Beppu–Shimabara graben structure¹⁷⁾ in the central Kyushu Island, Southwest Japan. The first event ($M_{\text{JMA}}6.5$ on the Japan Meteorological Agency scale) occurred along the Hinagu fault zone at 21:26 (JST) on April 14, 2016, followed by the second event ($M_{\text{JMA}}6.4$) that occurred 10 km to the south of the Hinagu fault zone at 0:03 on April 15, 2016. The largest event ($M_{\text{JMA}}7.3$) struck along the Futagawa fault zone at 1:25 on April 16, 2016 (Fig. 1), which was close to the

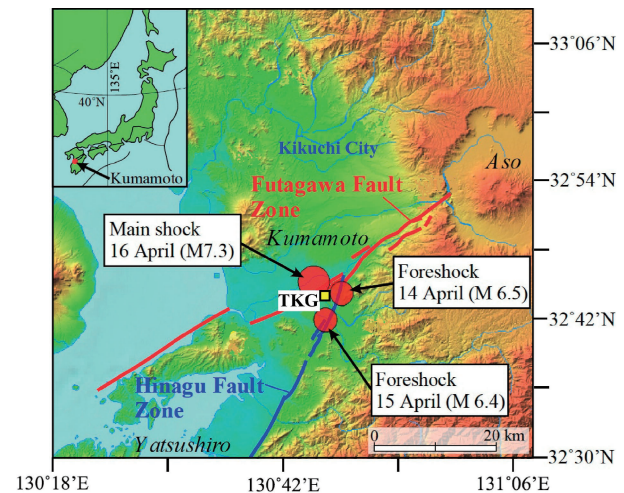


Fig. 1. Sampling site “Takagi” (TKG) of deep groundwater in the Kumamoto region in Southwest Japan together with epicenters of two foreshocks ($M_{\text{JMA}}6.5$ and $M_{\text{JMA}}6.4$) and the main shock ($M_{\text{JMA}}7.3$) of the 2016 Kumamoto earthquake. Red and blue curves show the Futagawa and Hinagu fault zones, respectively. The inset map shows the location of the Kumamoto region in Japan.

two previously mentioned foreshock locations. Its focal mechanism was strike–slip faulting with NW–SE tension, and the focal depth was approximately 10 km. This earthquake sequence resulted in 50 fatalities and injured more than 1,800 people; further, it considerably damaged the local infrastructure.

The Kumamoto region is characterized by active groundwater flows within the Quaternary sedimentary basin at which two major aquifer systems exist in a vertically separated manner.¹⁸⁾ These aquifer systems comprise a shallow unconfined aquifer with a depth of ~50 m and a deep confined aquifer with a depth of 60–200 m. Both the aquifers may have recharged owing to the highly permeable sediments in the northern and eastern hills, and groundwater would flow southward and westward along the topographical gradient.¹⁸⁾ The production well of mineral water samples (Takagi site) was located in Mifune Town, Kumamoto Prefecture, 3 km to the southeast of the epicenter of the main shock and at approximately the center of a triangle made by the three aforementioned large events (Fig. 1). This is one of the monitoring stations located closer to the epicenter of a large-magnitude earthquake from among the numerous case histories described in scientific literature.¹⁹⁾ The aquifer is estimated to be approximately 150-m deep and comprises sandstone, conglomerate, and red mudstone; it presumably belongs to the Upper Cretaceous Mifune Group.^{20),21)} We collected four sedimentary rocks that may be present in the aquifer, which is exposed 2.5 km to the northeast of the Takagi site,²¹⁾ and measured their oxygen isotopic compositions ($\delta^{17}\text{O}$ and $\delta^{18}\text{O}$ values). The oxygen isotopic composition was analyzed at the Korea Polar Research Institute using the automated laser fluorination technique.²²⁾ The observed data are presented in Table 1.

The groundwater samples were filtered and sealed in polyethylene terephthalate (PET) bottles and distributed in the market. We purchased as many bottles as possible covering a period of up to

one year before and two years after the $M_{\text{JMA}}7.3$ earthquake. The hydrogen and oxygen isotopes of the water samples were evaluated via cavity ring-down spectroscopy (L2120-I Analyzer; PICARRO Co. Ltd., California) at the Atmosphere and Ocean Research Institute, The University of Tokyo, without performing any chemical preprocessing. The observed hydrogen and oxygen isotopic ratios were calibrated against our inhouse standard and converted into the conventional V-SMOW scale (per mil (‰)). The instrumental errors associated with the $\delta^{18}\text{O}$ and $\delta^2\text{H}$ values were less than 0.12‰ and 0.6‰, respectively, at 2σ ; these values were estimated by repeatedly evaluating our inhouse standard. The experimental details are given elsewhere.¹⁵⁾

3. Results

The secular variation of the $^{18}\text{O}/^{16}\text{O}$ ratios associated with the Takagi groundwater from April 24, 2015 to March 5, 2018 is shown in Fig. 2a, covering a time period of one year before and two years after the 2016 Kumamoto earthquake. There are 117 data points covering this three-year period, resulting in a sampling frequency of 3.3 samples per month; however, a mineral water company may produce samples every day. This sampling frequency and the time period covering all the earthquake events show no fragmental data in accordance with any critical assessment³⁾ (see Fig. 2). The $\delta^{18}\text{O}$ values decrease gradually from -5.6‰ in 2015 to -6.3‰ in 2018, except for some apparent outliers. The simple linear regression of data is indicated by a dashed line. The slope of the fitted line is $-0.21 \pm 0.03\text{‰/year}$ (2σ ; $n = 117$; correlation coefficient $r^2 = 0.787$; mean square weighted deviation [MSWD] = 0.45). Four outlier samples can be clearly observed from Fig. 2a. They are inconsistent with the trend observed with an uncertainty of 3σ and show positive $\delta^{18}\text{O}$ values, including the sample on January 7, 2016 obtained three months before the $M_{\text{JMA}}7.3$ earthquake and three consecutive samples obtained from May 9 to May 12, 2016 soon after the $M_{\text{JMA}}7.3$ earthquake. Even though this is a very simple data treatment, one may recognize that it is not anymore anecdotal. There are two more potential outliers (open squares), which will be discussed later. By observing the data more closely, a weak seasonal variation, high in $\delta^{18}\text{O}$ in summer and low in $\delta^{18}\text{O}$ in winter, can be observed. This can be probably attributed to the environmental conditions associated with the recharge area of the Takagi groundwater; this will be discussed later.

Table 1. The oxygen isotopic compositions of sedimentary rocks belonging to the Upper Cretaceous Mifune Group

Sample	$\delta^{17}\text{O}$ (‰)	2σ error (‰)	$\delta^{18}\text{O}$ (‰)	2σ error (‰)
MFU-1	7.24	0.19	13.88	0.38
MFU-2	7.80	0.17	14.97	0.32
MFU-3	6.94	0.04	13.32	0.06
MFU-4	9.01	0.01	17.29	0.01

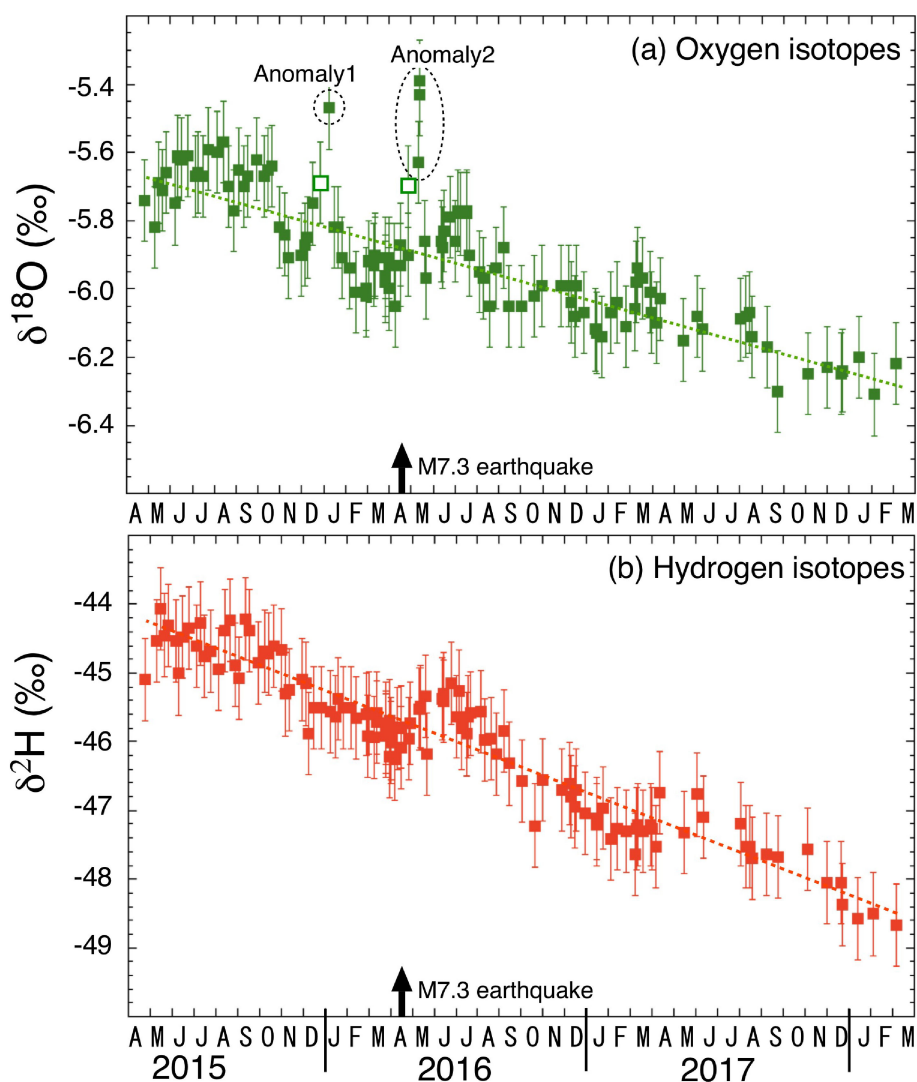


Fig. 2. (Color online) Secular variation of the (a) $\delta^{18}\text{O}$ values of deep groundwater and (b) $\delta^2\text{H}$ values at TKG site in the Kumamoto region. The error assigned to the symbol is 2σ bar. The arrow indicates the $M_{\text{JMA}}7.3$ earthquake event's date. The dashed line represents the simple linear regression through data. The oxygen data in dotted ovals are outliers with 3σ uncertainty off the trend. The open square samples are discussed in the section (4.1). There are no outliers within 3σ for the hydrogen isotopic data.

The temporal variation of the $^2\text{H}/\text{H}$ ratios is shown in Fig. 2b. The $\delta^2\text{H}$ values with a typical error of 0.6‰ at 2σ decrease from -44.2‰ in 2015 to -48.6‰ in 2018. A simple linear regression of the obtained data was performed and is indicated by a dashed line. The slope of the fitted line is $-1.46 \pm 0.09\text{‰}/\text{year}$ (2σ , $r^2 = 0.908$, $\text{MSWD} = 0.11$), approximately seven times steeper than that of oxygen. A better fitting, with high r^2 and low MSWD than those of oxygen, was also obtained. There are no outliers of hydrogen isotopes based on the trend observed with an uncertainty of 3σ . Again, a very slight seasonal variation can be observed relative

to the fitted line in Fig. 2b. The general decreasing trend of $\delta^{18}\text{O}$ and $\delta^2\text{H}$ with time will be discussed below.

4. Discussion

4.1. Mechanism of oxygen and hydrogen isotope changes. Groundwater is mainly derived from meteoric water, including precipitation (snow and rain), and river and lake water in temperate and humid climates.^{23),24)} A minor part of groundwater can be attributed to the water trapped in sediments (connate water) and the water obtained from magmatic sources. The origin and evolution of

meteoric water were discussed based on the oxygen and hydrogen isotopes.²⁵⁾ We follow the isotope method and discuss the groundwater characteristics based on these isotopes. Generally, the oxygen and hydrogen isotopes exhibit a decreasing trend with time (Figs. 2a and 2b, respectively). These variations may be caused by a common physicochemical mechanism. The seasonal variation of meteoric water is attenuated during transit and storage in the deep aquifer.²³⁾ This should be the case of the present samples. The decrease in the $\delta^{18}\text{O}$ and $\delta^2\text{H}$ values may be attributed to the continuous pumping of groundwater from the production well (a few tons per day) for producing mineral water even though there is no detailed geohydrological description of the well. The binary mixing of different water masses or isotopic fractionation during fluid flow may be induced by tapping a large amount of water. If the volume of the aquifer is considerably larger than that of the water pumped daily, a constant decrease in oxygen and hydrogen isotopes may be observed because of the steady state supply of water with low $\delta^{18}\text{O}$ and $\delta^2\text{H}$ values from a hidden second aquifer. This is the simple and dynamic mixing process of groundwater. However, this cannot be attributed to the local crustal deformation because the rate of change is very constant; the local crustal deformation remains constant for three years. The other candidate is the isotopic fractionation caused

by filtration through clay minerals in an aquifer during the induced fluid flow. The porewater obtained by filtration through clay minerals may contain enriched heavy isotopes of oxygen and hydrogen.²⁵⁾ Then, the filtered water may become lighter than the original water, and the $\delta^{18}\text{O}$ and $\delta^2\text{H}$ values may decrease with time, as observed in Fig. 2.

When the stable isotopes of global water are plotted together in the so-called Craig's diagram, a linear relation can be observed between the $\delta^{18}\text{O}$ and $\delta^2\text{H}$ values with a slope of 8.^{26),27)} The line denoting this linear relation is called the global meteoric water line (GMWL). Further, this linear relation can be mainly attributed to the isotopic fractionation caused by the evaporation and condensation of water at different latitudes. The groundwater samples are also characterized by their signatures in Craig's $\delta^{18}\text{O}$ – $\delta^2\text{H}$ diagram.^{25),27)} The relation between the $\delta^{18}\text{O}$ and $\delta^2\text{H}$ values associated with the monthly precipitation in the Kumamoto region²⁸⁾ is presented in Fig. 3a together with deep groundwater at the Takagi site. The rainwater during the summer (June–September) shows significantly smaller $\delta^{18}\text{O}$ and $\delta^2\text{H}$ values than that during winter (December–March). In addition, the variations of both the isotopes are much larger than those of the groundwater samples. Figure 3b shows the relation between the $\delta^{18}\text{O}$ and $\delta^2\text{H}$ values with respect to the Takagi groundwater samples, which can be obtained by enlarging a part of Fig. 3a.

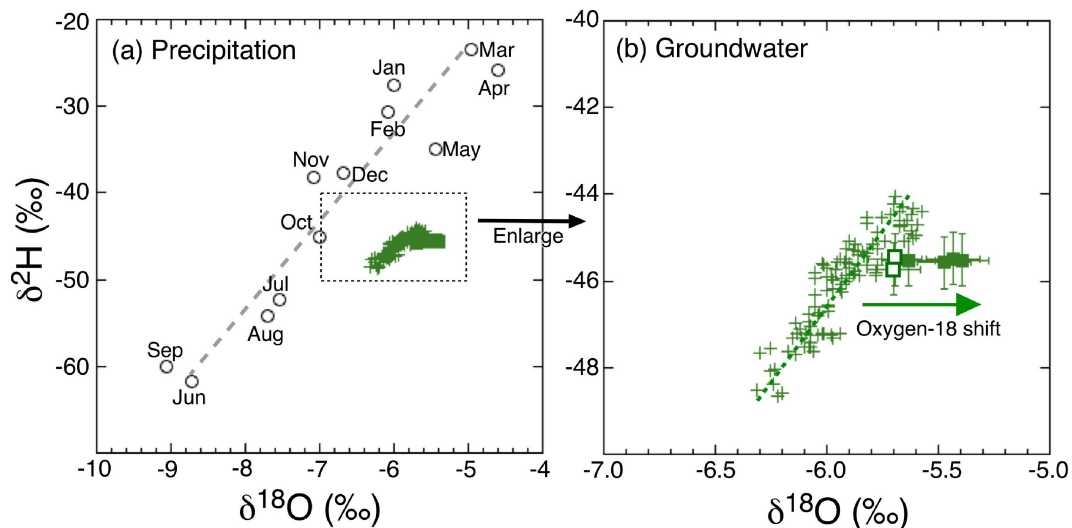


Fig. 3. (Color online) (a) Relation between the $\delta^{18}\text{O}$ and $\delta^2\text{H}$ values of monthly precipitation in the Kumamoto region²⁸⁾ together with deep groundwater at TKG site. The general trend is shown by a dashed line. (b) Relation between the $\delta^{18}\text{O}$ and $\delta^2\text{H}$ values of the groundwater. A part of Fig. 3a is enlarged. The arrow indicates the samples showing $\delta^{18}\text{O}$ anomaly without $\delta^2\text{H}$ change, possibly due to the oxygen-18 shift. Four solid squares are outliers with 3σ off the trend in Fig. 2a. Two open squares are 2σ from the dashed line. The error bar assigned to the symbol is 2σ .

Four outliers with significantly high $\delta^{18}\text{O}$ values are excluded (there are 3σ outliers in Fig. 2a), and the simple linear regression of data is indicated by a dashed line in Fig. 3b. The slope of the fitted line is 5.80 ± 0.51 (2σ , $r^2 = 0.824$, and $\text{MSWD} = 0.22$), which is slightly less than the value of seven independently calculated from the data obtained from Figs. 2a and 2b. The aforementioned slope is also smaller than the value of eight observed in case of GMWL because of the evaporation and condensation observed in the equilibrium condition²⁶; this can be probably attributed to the mixing of different types of water or isotopic fractionation during fluid flow owing to the continuous pumping of groundwater. A hypothetically hidden second aquifer may have been formed owing to the summer precipitation in the region (Fig. 3a), and their $\delta^{18}\text{O}$ and $\delta^2\text{H}$ values may be smaller than those of the Takagi water. A shallow unconfined aquifer may contribute to the formation of a second aquifer. However, the older age of the second water inferred by attenuation of seasonal variation should conflict with the shallow and thus young origin. Tritium–helium-3 dating of the samples should be conducted to resolve this problem.

In the $\delta^{18}\text{O}$ – $\delta^2\text{H}$ diagram (Fig. 3b), two outliers with relatively high $\delta^{18}\text{O}$ values (open square symbol in Fig. 2a) can be observed along with four outliers (solid squares). One sample was collected on December 25, 2015, approximately two weeks before the occurrence of anomaly 1 (see Fig. 2a). The other sample was collected on April 26, 2016, approximately two weeks before the occurrence of anomaly 2. These two samples are located just before the outliers obtained with an uncertainty of 3σ (solid squares) in the time sequence. Therefore, these two samples may be related to the anomalous events. Thus, there are six outlier samples, *i.e.*, two samples collected four months before the occurrence of the $M_{\text{JMA}7.3}$ earthquake and four consecutive samples obtained from April 26 to May 12, 2016 soon after the occurrence of the $M_{\text{JMA}7.3}$ earthquake. However, no corresponding outlier samples can be observed in case of hydrogen isotopes (Fig. 2b). Therefore, only an oxygen isotope anomaly could be observed. In case of the Tottori earthquake, a significant oxygen isotopic anomaly of $+0.24\text{‰}$ relative to the local background in groundwater was observed some months before the $M_{\text{JMA}6.6}$ earthquake.¹⁵ Further, a small but significant increase of 0.07‰ was observed soon after the earthquake. Because the $\delta^{18}\text{O}$ values of the water samples are approximately

-8.2‰ , which are considerably lower than the value of $+8.4\text{‰}$ measured for the aquifer rocks in the Tottori region, the groundwater $\delta^{18}\text{O}$ values may increase owing to the progressive equilibration of the oxygen isotope with the rocks.¹⁵ However, the $\delta^2\text{H}$ values of groundwater remain unchanged because the hydrogen content of the aquifer rocks is significantly low compared to the oxygen content. A similar mechanism based on the isotopic exchange of oxygen between the aquifer rocks and groundwater can be assumed in case of the Kumamoto earthquake (^{18}O shift in Fig. 3). There is another mechanism to change oxygen isotopes without changing the hydrogen isotope, *i.e.*, via exchange of oxygen isotopes between CO_2 and H_2O in natural CO_2 -rich spring water.²⁹ Generally, springs contain abundant CO_2 bubbling gas, indicating higher CO_2 content than the solubility of 40 mmol/L at 20°C . Further, we did not measure the total carbonate content of the samples; therefore, it is difficult to compare them directly. However, a study has investigated the chemical compositions of the groundwater in the Kumamoto region.³⁰ The groundwater close to our location indicated a CO_2 content of 0.02 mmol/L , which is at least three orders of magnitude smaller than the content of CO_2 bubbling gas. Therefore, the variation of oxygen isotopes because of CO_2 – H_2O exchange may be negligibly small.

The aquifer rocks belong to the Upper Cretaceous Mifune Group.^{20,21} Their $\delta^{18}\text{O}$ values vary from $+13.3\text{‰}$ to $+17.3\text{‰}$ (Table 1). Generally, these values are consistent with the $\delta^{18}\text{O}$ values of the Upper Cretaceous and Paleogene sedimentary rocks in the Amakusa area located 70 km to the southwest of the Kumamoto city, ranging from $+13.1\text{‰}$ to $+15.8\text{‰}$.³¹ The oxygen isotope data of the Cretaceous–Paleogene granitoids in the Kumamoto region show $\delta^{18}\text{O}$ values of $+9.1\text{‰}$ to $+12.6\text{‰}$,³² which is slightly smaller than the values associated with the present samples. Because the $\delta^{18}\text{O}$ values of the Takagi aquifer rocks are significantly higher than those of groundwater, an isotopic exchange of oxygen would increase the $\delta^{18}\text{O}$ values of the groundwater in the Kumamoto region, similar to that observed in the Tottori case study in which the reaction was very fast.¹⁵ The crustal deformation related to the 2016 Kumamoto earthquake may have enhanced the water–rock interaction in the 150-m -deep aquifer because of microfracturing. Therefore, the most probable mechanism to cause $\delta^{18}\text{O}$ enrichment is the ^{18}O shift caused by water–rock interaction¹⁶ without any $\delta^2\text{H}$ changes. A water–rock interaction

Table 2. The groundwater oxygen isotope anomaly caused by earthquakes

Location	Grimsey lineament, Northern Iceland	Husavik–Flatey Fault & Grimsey lineament, Northern Iceland	Tottori, Southwest Japan	Kumamoto, Southwest Japan
Magnitude	M5.8	M5.6 & M5.5	M _{JMA} 6.6	M _{JMA} 7.3
Depth	10 km	6 & 10 km	10 km	10 km
Date	September 16, 2002	October 21, 2012 & April 2, 2013	October 21, 2016	April 16, 2016
Distance	90 km	76 & 76 km	5 km	3 km
Strain change	<tidal stress	<tidal stress	3.3×10^{-6}	4.5×10^{-5}
Anomaly	$\delta^2\text{H}$ & $\delta^{18}\text{O}$	$\delta^2\text{H}$ & $\delta^{18}\text{O}$	$\delta^{18}\text{O}$	$\delta^{18}\text{O}$
Mechanism	Mixing of groundwater	Mixing of groundwater	Water–rock interaction	Water–rock interaction
Reference	Claesson <i>et al.</i> (2004) ¹²⁾	Skelton <i>et al.</i> (2014) ¹⁴⁾	Onda <i>et al.</i> (2018) ¹⁵⁾	This work

may have occurred in the second aquifer at the time of the Kumamoto earthquake even though we do not have clear evidence of this occurrence.

4.2. Difference between the groundwater anomalies of Japan and Iceland. Two case studies have been conducted in Iceland, in which both the $\delta^2\text{H}$ and $\delta^{18}\text{O}$ values of groundwater changed before and after the occurrence of earthquakes.^{12),14)} These data are compared with those obtained from this study and those obtained based on the 2016 Tottori earthquake (Table 2). All the events reported in the table are interplate earthquakes with epicenter depths of approximately 10 km and a strike–slip fault-type mechanism. However, the magnitudes of these earthquakes differ significantly. The magnitudes of the earthquakes in Iceland are from M5.5 to M5.8, whereas those of the earthquakes in Japan are M_{JMA}6.6 and M_{JMA}7.3. This indicates that the rapture energy in Japan is two orders of magnitude greater than that in Iceland. The empirical relation between the magnitude of an earthquake and the volume of crustal rock affected by the seismic activity was expressed as follows³³⁾:

$$\log V = 1.06 M - 2.78, \quad [1]$$

where V and M denote the affected volume of rock in km^3 and the magnitude, respectively. In case of the Kobe earthquake that occurred in central Japan on January 17, 1995, the magnitude of the earthquake was converted into the volume of rock and the related helium degassing was considered.³⁴⁾ In case of Iceland, the volume of affected rock becomes $1,600 \text{ km}^3$ when the values obtained from the two

earthquakes, M5.5 and M5.8, are averaged. Further, the volume is $39,000 \text{ km}^3$ in Japan, which is considerably larger than that of Iceland. In addition, the distances from the epicenters and the groundwater monitoring stations are different for the cases. The monitoring stations in Iceland are 76 and 90 km away from the epicenter, whereas those in Japan are only 3 and 5 km away from the epicenter of the Kumamoto and Tottori earthquakes, respectively.

Consequently, the estimated coseismic volumetric strain change is discrepant in case of Iceland and Japan. The strain changes are possibly less than the tidal stress at the monitoring station in Iceland,^{12),14)} and high strain changes of 3.3×10^{-6} and 4.5×10^{-5} in the Tottori and Kumamoto stations, respectively, were calculated using a finite fault model³⁵⁾ and explained later. The proposed groundwater anomaly mechanism is also different between Iceland and Japan. In case of Iceland, the $\delta^2\text{H}$ and $\delta^{18}\text{O}$ values changed; further, these values can be attributed to the mixing of groundwater from different isotopic signatures.^{12),14)} In case of Japan, only the $\delta^{18}\text{O}$ values increased and the $\delta^2\text{H}$ values did not exhibit any considerable change. This peculiar behavior may be caused by the water–rock interaction, which will be discussed in detail later. If the anomalies in Iceland can be attributed to the strain changes induced by crustal deformation, unusual and/or local enhancement of chemical and isotopic variation for a tiny change in strain would be required to explain these anomalies. In any case, we cannot deny the crustal deformation hypothesis in Iceland at present, and the difference of mechanism may be attributed to

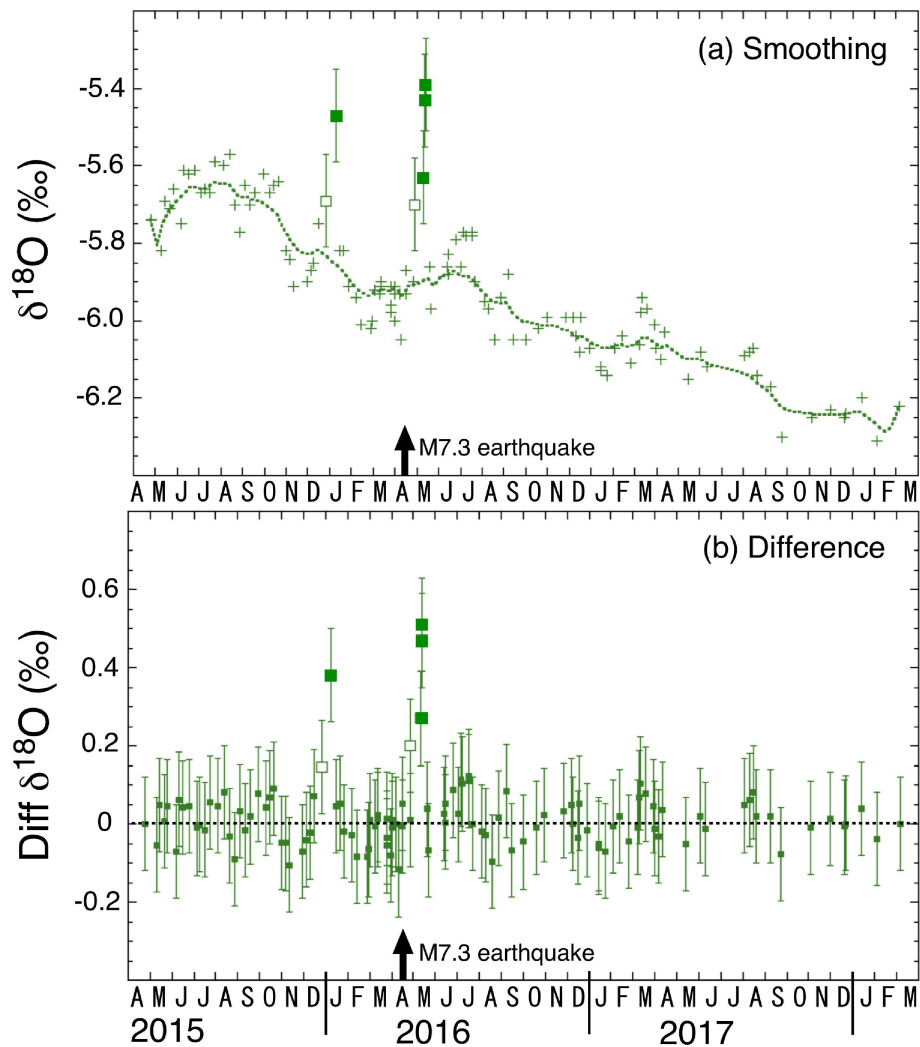


Fig. 4. (Color online) Smoothing data of the (a) secular variation of the $\delta^{18}\text{O}$ values of deep groundwater at the TKG site in the Kumamoto region. Six outliers are shown by squares with 2σ error bars. The arrow indicates the $M_{\text{JMA}}7.3$ earthquake event. The general trend is shown by a dotted curve. (b) Difference between the original and smoothed $\delta^{18}\text{O}$ data of deep groundwater. The arrow indicates the $M_{\text{JMA}}7.3$ earthquake event.

a location-specific problem or the geological conditions of the monitoring site. This should be resolved in future research.

4.3. $\delta^{18}\text{O}$ anomaly and coseismic strain changes. To discuss the $\delta^{18}\text{O}$ anomaly in case of groundwater in a quantitative manner and its relation with the volumetric strain changes during an earthquake, the $\delta^{18}\text{O}$ shift should be precisely calculated in a numerical manner. Based on the aforementioned discussion, we masked the six outlier samples (solid squares in dotted oval and open squares in Figs. 2a and 3, respectively) from 117 $\delta^{18}\text{O}$ data and calculated the general trend and/or background variation via a simple moving average

method using all data points, except the six outliers. The smoothed data sequence is expressed in a dotted curve in Fig. 4a. The outliers are denoted using two open squares and four solid squares with experimental error bars of 2σ . The general trend (dotted curve) indicates a seasonal variation (high $\delta^{18}\text{O}$ in summer and low $\delta^{18}\text{O}$ in winter). This is explained by the isotopic variations in precipitation and groundwater in Japan.^{24),28)} The value called *d-excess*, which is defined as $\delta^2\text{H} - 8 \times \delta^{18}\text{O}$, in case of rain in Japan shows low values in summer (June–August) and high values in winter (December–February).²⁸⁾ Therefore, the $\delta^{18}\text{O}$ values of precipitation are higher in summer and lower in winter (Fig. 2a). This estimation can

explain the general trend of the $\delta^{18}\text{O}$ value in Fig. 4a. In addition, the amplitude of the seasonal variation becomes smaller with time, which can be attributed to the mixing of the studied groundwater with that originating from a hidden second aquifer, as stated in the previous section. The second reservoir may be older than the first reservoir, and the seasonal variation may have been attenuated during water storage in the aquifer.²³⁾

The difference between the $\delta^{18}\text{O}$ values with respect to the observed and smoothed data is plotted against the sampling date in Fig. 4b. Except for the six outlier samples (two open squares and four solid squares) with high $\delta^{18}\text{O}$ values, all the data are consistent with zero difference within an experimental error of 2σ . Further, the excess $\delta^{18}\text{O}$ values in this diagram can be calculated. They are 0.38‰ higher 3–4 months before the $M_{\text{JMA}}7.3$ event and 0.51‰ higher soon after the event when compared with the normal values.

Initially, we quantitatively discuss the physico-chemical mechanism responsible for the $\delta^{18}\text{O}$ anomaly after the 2016 Kumamoto earthquake ($M_{\text{JMA}}7.3$) along with that responsible for the 2016 Tottori earthquake ($M_{\text{JMA}}6.6$). During the latter event, a small but substantial increase of the $\delta^{18}\text{O}$ value, $0.070 \pm 0.055\text{‰}$ (2σ), was observed.¹⁵⁾ When the water–rock interaction is the driving mechanism of these $\delta^{18}\text{O}$ anomalies, the coseismic volumetric strain changes that induce the microfracturing of the local aquifer rocks should be considered. The strain change during an earthquake can be calculated using the finite fault model.³⁵⁾ The finite fault provides the modeled presentation of the spatial extent, amplitude, and duration of fault rupture (slip) of an earthquake based on the signature of the earthquake source fault, where the fault plane estimated by a geodetic model using the SAR method³⁶⁾ is different from that calculated by the inversion of strong motion data.³⁷⁾ Subsequently, we average the strain data obtained using the SAR method and the inversion method at the Takagi site during the Kumamoto earthquake. We also performed this calculation at the Hakusan Meisui site located approximately 5 km to the west of the Tottori earthquake epicenter.^{38),39)} The obtained volumetric strain changes are 4.5×10^{-5} in Kumamoto and 3.3×10^{-6} in Tottori, as presented in Table 2. Figure 5 shows the relation between the volumetric strain change and the increase in $\delta^{18}\text{O}$ value after the earthquake. There are only two data points available, among which one is for the Tottori earthquake¹⁵⁾ and

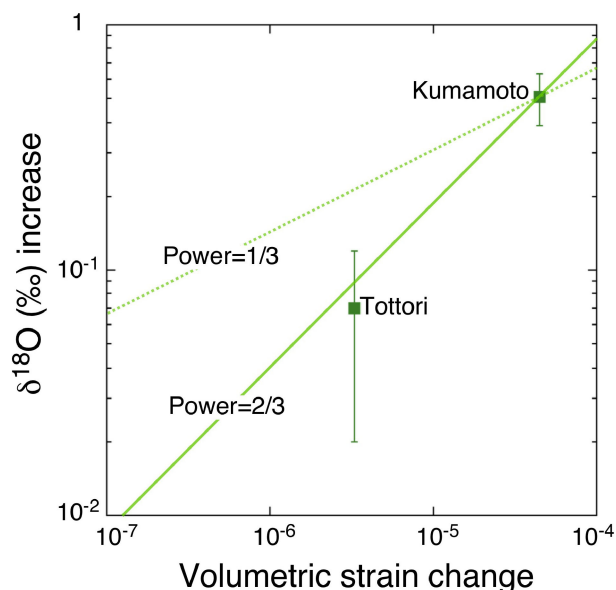


Fig. 5. (Color online) Relation between the coseismic volumetric strain change and $\delta^{18}\text{O}$ anomaly observed in the 2016 Tottori ($M_{\text{JMA}}6.6$) and 2016 Kumamoto earthquake ($M_{\text{JMA}}7.3$). The 2/3 power law (solid line) shows much better fit to the data than the 1/3 power law (dotted line).

the other is for the Kumamoto earthquake, as obtained from this study. The diagram is a double logarithmic diagram; therefore, the slope of the lines indicates the power of data on the X-axis using $Y = aX^b$, where b is the power. We tentatively draw two lines with $b = 1/3$ (dotted line) and $b = 2/3$ (solid line). The latter line was drawn to allow it to pass through the Kumamoto data point. The solid line is a better fit to the Tottori data point than the dotted line. Therefore, the power law of $b = 2/3$ should have a plausible geochemical implication even though there are only two data points.

4.4. Helium degassing experiments: microfracturing and the 2/3 power law. To explain the occurrence of noble gas emanation prior to seismic events,⁵⁾ helium degassing during rock fracturing was experimentally studied in the 1980s.⁴⁰⁾ The pioneering work⁴⁰⁾ was conducted in a laboratory to measure the variation of the helium contents in rocks subjected to uniaxial compression. The volume of the rock (V) underwent an inelastic increase (ΔV) because of the formation of microcracks when the rock was compressed. New cracks will form at the grain boundary with the increasing $\Delta V/V$ value. An increase of the total surface area of a rock will occur by new surfaces created by microfracturing. Consequently, the helium in the rock may be liberated

from the newly exposed surfaces. Then, the relation between the volumetric strain change ($\Delta V/V$) and the amount of helium released (v) can be expressed as follows⁴⁰⁾:

$$v = k_1 \times (\Delta V/V)^{2/3}, \quad [2]$$

where k_1 is a constant. This physicochemical relation should be observed during a seismic event. Soon after the 2016 Kumamoto earthquake, we collected deep groundwater samples from seven different sites around the Futagawa–Hinagu fault zones and measured their helium isotopic ratios ($^3\text{He}/^4\text{He}$) via noble gas mass spectrometry.⁶⁾ The helium data were compared with those obtained in August 2010.⁴¹⁾ The helium isotopic ratio clearly decreased at the site close to the Futagawa–Hinagu fault zones in Fig. 2 of our published paper.⁶⁾ Because the changes in the $^3\text{He}/^4\text{He}$ ratio were caused by degassing and the addition of radiogenic helium (^4He) accumulated in aquifer rocks during an earthquake, the volumetric strain change can be estimated using Eq. [2]. This was successfully conducted, and a linear relation was obtained between the amount of helium degassed and the volumetric strain change estimated by the fault model.³⁵⁾ Equation [2] was well fitted into the data distribution in a double logarithmic chart, resulting in the first quantitative coupling of laboratory experiment⁴⁰⁾ with field observations.⁶⁾ Recently, continental degassing of helium was observed in an active tectonic setting in northern Italy, and it was discussed with micro-fracturation of rocks.⁴²⁾

The geochemical implication of the 2/3 power law in Fig. 5 is supported by the relation between the rock fracturing experiments and the changes in helium isotopic ratios in the field. Even though there are only two data points in the figure, the proposed physicochemical mechanism for observing the $\delta^{18}\text{O}$ anomaly in case of groundwater is promising when new data points are provided after the occurrence of large-magnitude earthquakes. If the power of 2/3 in the relation between $\delta^{18}\text{O}$ enrichment (ω) and volumetric strain change ($\Delta V/V$) is appropriate, a best fit line passing through the two data points in Fig. 5 can be obtained as follows:

$$\omega = 390 \times (\Delta V/V)^{2/3}. \quad [3]$$

Based on Eq. [3], the relation between $\delta^{18}\text{O}$ enrichment and strain changes can be calculated. This is an innovative attempt to quantify the volumetric strain change using geochemical data.

4.5. Precursory anomaly of oxygen isotopes.

As stated in the previous section, a $\delta^{18}\text{O}$ enrichment

(or increase) of 0.38‰ relative to the background was observed 3–4 months prior to the occurrence of the Kumamoto $M_{\text{JMA}}7.3$ event (Fig. 4b), even though there is only one datum and we cannot completely eliminate the possibility that this may be an experimental artifact. In any case, the increase in $\delta^{18}\text{O}$ can be converted into a hypothetical volumetric strain change of 3.0×10^{-5} using Eq. [2], which is considerably larger than the tidal stress in the order of 1×10^{-8} in the region. Unfortunately, the bore-hole-type volumetric strain meter is not located close to the Takagi site, where the groundwater samples are collected. It is difficult to verify the supposed volumetric strain change based on field geophysical observations.

Instead of the strain change, other precursor signals were reported as follows. A preseismic ionospheric anomaly was observed before the 2016 Kumamoto earthquake by the global navigation satellite system.⁴³⁾ However, this could be observed several tens of minutes before the $M_{\text{JMA}}7.3$ event and is not related with the $\delta^{18}\text{O}$ anomaly observed 3–4 months before the earthquake. Abnormal gravity wave activity could also be observed in the stratosphere prior to the $M_{\text{JMA}}7.3$ event.⁴⁴⁾ Again, this occurred approximately one week before the earthquake and was not related to the $\delta^{18}\text{O}$ anomaly. Precursory seismic patterns prior to the $M_{\text{JMA}}7.3$ event were reported by four different methods (b -value method, two methods of seismic quiescence evaluation, and an analysis of seismic density in space and time).⁴⁵⁾ The precursory phenomena durations were either 1.5 or 3 years and much longer than the 3–4-month period considered in this study. Therefore, none of the reported preseismic anomalies match our observation in the time sequence. Instead of these signals, small but substantial seismic swarm activities were observed in Kikuchi City, Kumamoto region.⁴⁶⁾ The activity began in the middle of November 2015 and continued until the second week of December 2015, including the period when $M_{\text{JMA}}3.2$ and $M_{\text{JMA}}3.1$ events occurred on December 4 and 7, respectively. They were shallow crustal earthquakes with depths of 5–6 km and epicenters located approximately 20 km to the north of the groundwater monitoring site (TKG in Fig. 1) in Mifune Town. The timing is consistent with the period of the observed oxygen anomalies on December 25, 2015 and January 7, 2016. The time lag of 18 days is not considerably different from that of 10 days between the $M_{\text{JMA}}7.3$ event (April 16) and the initiation of the oxygen anomaly (April 26). However, these earth-

quakes were so small and far from the TKG monitoring site that the coseismic strain changes may not produce the supposed change of 3.0×10^{-5} calculated by Eq. [2]. A possible scenario is that a nondestructive and very slow preslip of Futagawa fault may have been induced by the earthquakes in Kikuchi City (the $M_{\text{JMA}}3.1$ and $M_{\text{JMA}}3.2$ events) because the area was highly stressed at the time, as indicated by the low b -value.⁴⁵⁾ The hypothesis should be challenged by a future geodetic study.

5. Conclusion

Critical reviews of earthquake prediction studies reported that majority of the precursory data were anecdotal or fragmental. Further, knowledge about the mechanism associated with the formation of such geochemical anomalies is lacking. To meet the criteria for assessing geochemical anomalies, we have measured 117 oxygen and hydrogen isotopes in the groundwater samples collected from a monitoring well located in Mifune Town, Kumamoto Prefecture. The period was from April 24, 2015 to March 5, 2018, with the 2016 Kumamoto earthquake in Southwest Japan during the period. The samples were obtained during a period of one year before and two years after the $M_{\text{JMA}}7.3$ earthquake events of April 16 with an approximate sampling frequency of 3.3 samples per month. The background variations of $^{18}\text{O}/^{16}\text{O}$ and $^2\text{H}/\text{H}$ ratios monotonically decreased with time and exhibited a slight seasonal variation. After simple statistical treatment of the data, a couple of positive $\delta^{18}\text{O}$ anomalies (six samples in total) could be observed 3–4 months before and soon after the $M_{\text{JMA}}7.3$ event. However, there were no outliers with respect to the measured $\delta^2\text{H}$ values. The crustal movement and rupture during the earthquake may have increased the microfracturing of the aquifer rocks. The enhanced water–rock interaction on the increased surface area of rocks may have induced oxygen exchange between water and rock, increasing the $\delta^{18}\text{O}$ value without affecting $\delta^2\text{H}$. Considering the $\delta^{18}\text{O}$ anomaly observed after the $M_{\text{JMA}}7.3$ earthquake along with that observed after the 2016 Tottori earthquake, a quantitative relation can be extracted between the increased $\delta^{18}\text{O}$ values and volumetric strain change with a 2/3 power law. This is the first quantitative relation between geochemical and geophysical data during a great/big earthquake; further, more case studies should be conducted in future. Thus, the groundwater oxygen isotopes may be considered as an effective strain gauge.

Acknowledgments

We gratefully acknowledge the anonymous mineral water company for providing several water samples. We are thankful to Prof. N. Koizumi for the discussion on chemical precursors and two anonymous referees for constructive reviews. This study was partly supported by the Ministry of Education, Culture, Sports, Science and Technology (MEXT) of Japan, under its Earthquake and Volcano Hazards Observation and Research Program, and by a research grant from the Japan Society for the Promotion of Science (17H00777). The laser fluorination oxygen isotope analysis was funded by the Korea Polar Research Institute (PE20200).

References

- 1) King, C., Koizumi, N. and Kitagawa, Y. (1995) Hydrogeochemical anomalies and the 1995 Kobe earthquake. *Science* **269**, 38–39.
- 2) Ingebritsen, S.E. and Manga, M. (2014) Hydrogeochemical precursors. *Nat. Geosci.* **7**, 697–698.
- 3) Roeloff, E. (1988) Hydrologic precursors to earthquakes: A review. *Pure Appl. Geophys.* **126**, 177–209.
- 4) Barberio, M.D., Barbieri, M., Billi, A., Doglioni, C. and Petitta, M. (2017) Hydrogeochemical changes before and during the 2016 Amatrice-Norcia seismic sequence (central Italy). *Sci. Rep.* **7**, 11735.
- 5) Sugisaki, R. and Sugiura, T. (1985) Geochemical indicator of tectonic stress resulting in an Earthquake in central Japan. *Science* **229**, 1261–1262.
- 6) Sano, Y., Takahata, N., Kagoshima, T., Shibata, T., Onoue, T. and Zhao, D. (2016) Groundwater helium anomaly reflects strain change during the 2016 Kumamoto earthquake in Southwest Japan. *Sci. Rep.* **6**, 37939.
- 7) Sugisaki, R. (1978) Changing He/Ar and N_2/Ar ratios of fault air may be earthquake precursors. *Nature* **275**, 209–211.
- 8) Wakita, H., Nakamura, Y., Notsu, K., Noguchi, M. and Asada, T. (1980) Radon anomaly, a possible precursor of the 1978 Izu-Oshima-Kinkai earthquake. *Science* **207**, 882–883.
- 9) Geller, R.J. (1997) Earthquake prediction: A critical review. *Geophys. J. Int.* **131**, 425–450.
- 10) Tsunogai, U. and Wakita, H. (1995) Precursory chemical changes in ground water: Kobe earthquake, Japan. *Science* **269**, 61–63.
- 11) O’Neil, J.R. and King, C. (1981) Variations in stable-isotope ratios of ground waters in seismically active regions of California. *Geophys. Res. Lett.* **8**, 429–432.
- 12) Claesson, L., Skelton, A., Graham, C., Dietl, C., Morth, M., Torssander, P. *et al.* (2004) Hydrogeochemical changes before and after a major earthquake. *Geology* **32**, 641–644.
- 13) Reddy, D.V., Nagabhushanam, P. and Sukhija, B.S.

- (2011) Earthquake (M5.1) induced hydrogeochemical and $\delta^{18}\text{O}$ changes: Validation of aquifer breaching-mixing model in Koyna, India. *Geophys. J. Int.* **184**, 359–370.
- 14) Skelton, A., Andren, M., Kristmannsdottir, H., Stockmann, G., Morth, C.-M., Sveinbjornsdottir, A. *et al.* (2014) Changes in groundwater chemistry before two consecutive earthquakes in Iceland. *Nat. Geosci.* **7**, 752–756.
- 15) Onda, S., Sano, Y., Takahata, N., Kagoshima, T., Miyajima, T., Shibata, T. *et al.* (2018) Groundwater oxygen isotope anomaly before the M6.6 Tottori earthquake in Southwest Japan. *Sci. Rep.* **8**, 4800.
- 16) Craig, H. (1963) The isotopic geochemistry of water and carbon in geothermal areas. *In* Nuclear Geology on Geothermal Areas: Spoleto, 1963 (ed. Tongiorgi, E.). Consiglio Nazionale Delle Ricerche (CNR), Laboratorio Di Geologia Nucleare, Pisa, pp. 17–53.
- 17) Kato, A., Nakamura, K. and Hiyama, Y. (2016) The Kumamoto earthquake sequence. *Proc. Jpn. Acad. Ser. B* **92**, 358–371.
- 18) Geological Survey of Japan (2014) Water Environment Map Database, 7. Kumamoto Area. <https://gbank.gsj.jp/WaterEnvironmentMap/contents/kumamoto/kumamoto/Kumamoto.htm> (in Japanese).
- 19) Hartmann, J. and Levy, J.K. (2005) Hydrogeological and gasgeochemical earthquake precursors—A review for application. *Nat. Hazards* **34**, 279–304.
- 20) Kuroki, S., Okada, H. and Sakai, T. (1995) Sedimentary facies and environments of the Upper Cretaceous Mifune Group in the Axial Zone of Kyushu. *J. Sed. Soc. Jpn.* **41**, 65–83.
- 21) Nakayama, H. (2019) A Geological Cross Section of the Kumamoto Region. Kumanichi Publishing, Kumamoto (in Japanese).
- 22) Kim, N.K., Kusakabe, M., Park, C., Lee, J.I., Nagao, K., Enokido, Y. *et al.* (2019) An automated laser fluorination technique for high-precision analysis of three oxygen isotopes in silicates. *Rapid Commun. Mass Spectrom.* **33**, 641–649.
- 23) Gat, J.R. (1971) Comments on the stable isotope method in regional groundwater investigation. *Water Resour. Res.* **7**, 980–993.
- 24) Mizota, C. and Kusakabe, M. (1994) Spatial distribution of δD - $\delta^{18}\text{O}$ values of surface and shallow groundwaters from Japan, south Korea and east China. *Geochem. J.* **28**, 387–410.
- 25) Sakai, H. and Matsuhisa, Y. (1996) Stable Isotope Geochemistry. University of Tokyo Press, Tokyo (in Japanese).
- 26) Craig, H. (1961) Isotopic variations in meteoric waters. *Science* **133**, 1702–1703.
- 27) Hoefs, J. (2004) Stable Isotope Geochemistry (5th ed.). Springer, Berlin.
- 28) Tanoue, M., Ichiyanagi, K. and Shimada, J. (2009) Seasonal variation and short-term fluctuation of stable isotopes of precipitation in Kumamoto. *In* Abstract of the 2009 Autumn Meeting of Meteorological Society of Japan (Fukuoka, 2009). Meteorological Society of Japan, Tokyo, Abstract P122 (in Japanese).
- 29) Karolyte, R., Serno, S., Johnson, G. and Gilfillan, S.M.V. (2017) The influence of oxygen isotope exchange between CO_2 and H_2O in natural CO_2 -rich spring waters: Implications for geothermometry. *Appl. Geochem.* **84**, 173–186.
- 30) Kawagoshi, Y., Koga, H., Suenaga, Y., Hama, T. and Ito, H. (2018) Influence of the 2016 Kumamoto earthquake on groundwater quality. *Jpn. J. Limnol.* **79**, 147–158 (in Japanese).
- 31) Matsuhisa, Y. and Tohashi, Y. (1979) Oxygen, hydrogen and carbon isotopic study of the Amakusa pottery stone deposits in altered rhyolite dykes, Kyushu, southwest Japan. *Geochem. J.* **13**, 173–179.
- 32) Ishihara, S. and Matsuhisa, Y. (2002) Oxygen isotopic constraints on the genesis of the Cretaceous-Paleogene granitoids in the Inner Zone of Southwest Japan. *Bull. Geol. Survey Jpn.* **53**, 421–438.
- 33) Shimazu, Y. (1971) Physics of the Earth. Shokabo Press, Tokyo (in Japanese).
- 34) Sano, Y., Takahata, N., Igarashi, J., Koizumi, N. and Sturchio, N.C. (1998) Helium degassing related to the Kobe earthquake. *Chem. Geol.* **150**, 171–179.
- 35) Okada, Y. (1992) Internal deformation due to shear and tensile faults in a half-space. *Bull. Seismol. Soc. Am.* **82**, 1018–1040.
- 36) Yurai, H., Kobayashi, T., Morishita, Y., Fujiwara, S., Hiyama, Y., Kawamoto, S. *et al.* (2016) Source fault models of the 2016 Kumamoto earthquake inverted from crustal deformation. *J. GSI* **128**, 169–176 (in Japanese).
- 37) Kubo, H., Suzuki, W., Aoi, S. and Sekiguchi, H. (2016) Source rupture processes of the 2016 Kumamoto, Japan, earthquake estimated from strong-motion waveforms. *Earth Planets Space* **68**, 161.
- 38) Kubo, H., Suzuki, W., Aoi, S. and Sekiguchi, H. (2017) Source rupture process of the 2016 central Tottori, Japan, earthquake ($M_{\text{JMA}}6.6$) inferred from strong motion waveforms. *Earth Planets Space* **69**, 127.
- 39) Geospatial Information Authority of Japan (GSI) (2016) Source fault model of the 2016 central Tottori earthquake. <https://www.gsi.go.jp/BOUSAI/dansoumoderu.html> (in Japanese).
- 40) Honda, M., Kurita, K., Hamano, Y. and Ozima, M. (1982) Experimental studies of He and Ar degassing during rock fracturing. *Earth Planet. Sci. Lett.* **59**, 429–436.
- 41) Horiguchi, K. and Matsuda, J. (2013) Geographical distribution of $^3\text{He}/^4\text{He}$ ratios in north Kyushu, Japan: Geophysical implications for occurrence of mantle-derived fluids at deep crustal levels. *Chem. Geol.* **340**, 13–20.
- 42) Buttitta, D., Caracausi, A., Chiaraluce, L., Favara, R., Morticelli, M.G. and Sulli, A. (2020) Continental degassing of helium in an active tectonic setting (northern Italy): The role of seismicity. *Sci. Rep.* **10**, 162.

- 43) Iwata, T. and Umeno, K. (2016) Preseismic ionospheric anomalies detected before the 2016 Kumamoto earthquake. *J. Geophys. Res. Space Phys.* **122**, 3602–3616.
- 44) Yang, S.-S., Asano, T. and Hayakawa, M. (2019) Abnormal gravity wave activity in the stratosphere prior to the 2016 Kumamoto earthquakes. *J. Geophys. Res. Space Phys.* **124**, 1410–1425.
- 45) Nanjo, K.Z., Izutsu, J., Orihara, Y., Furuse, N., Togo, S., Nitta, H. *et al.* (2016) Seismicity prior to the 2016 Kumamoto earthquakes. *Earth Planets Space* **68**, 187.
- 46) Japan Meteorological Agency (JMA) (2015) Monthly report on earthquakes and volcanoes in Japan, December 2015. <https://www.data.jma.go.jp/svd/eqev/data/gaikyo/monthly/201512/201512index.html> (in Japanese).

(Received Mar. 27, 2020; accepted June 10, 2020)